

مدل سازی گسله‌های امتداد لغز

نوشته: حسن شهریور *

خلاصه

طبق تعریف (Sylvester 1988) گسله امتداد لغز گسله‌ای است که بیشتر حرکت آن به موازات راستای گسله است. این گسله‌ها بیش از هزار کیلومتر درازا داشته و میزان جابجایی آن‌ها نیز از چند میلی‌متر تا ده‌ها کیلومتر است. در یک محدودهٔ باریک می‌توان شکاف‌ها، گسله‌ها و چین‌های En-echelon را مشاهده کرد. افزون بر آن این گسله ساختمان‌هایی نظیر گسله‌ها، چین‌ها، دایک‌ها، سیلها و تورق‌ها را جابجا کرده و سنگ‌هایی با سن، جنس، رخساره و ساختمان مختلف را در کنار یکدیگر قرار می‌دهند.

در این گسله‌ها سه نوع ساختمان اصلی حاصل از کوتاه‌شدگی، انبساط و شیرینگ افقی پدید می‌آید. دو نوع مکانیزم شیرینگ محض و ساده، روابط هندسی و دینامیکی را در این گسله‌ها تشریح می‌کنند. بیشتر گسله‌های راست‌الغز در محدودهٔ شیرینگ ساده شکل می‌گیرند.

این گسله‌ها در آزمایشگاه‌های تکنیک تجربی توسط برپاداشتن مدل‌های مشابه مورد بررسی قرار گرفته‌اند. نتایج حاصله از بررسی مدل‌ها و رسوبات آبرفتی تغییر شکل یافته نشان می‌دهد که پنج نوع شکاف در اثر کارکرد این گسله‌ها به وجود می‌آید:

- ۱- شیرینگ‌های Riedel (R): که با محدودهٔ اصلی جابجایی (PDZ) زاویه‌ای حدود $\Phi/2$ می‌سازند.
- ۲- سطوح شیرینگ مکمل Riedel (R'): که تحت زاویه $90 - \Phi/2$ با (PDZ) پدید می‌آیند.
- ۳- شیرینگ‌های P: که تحت زاویه $\Phi/2$ با PDZ قرار دارند و جهت حرکتشان با گسل همسو است.
- ۴- شکاف‌های انبساطی T: که زاویه 45 درجه با PDZ دارند.
- ۵- گسله‌های موازی Y: که با PDZ موازی هستند.

در اینجا Φ زاویهٔ شکست داخلی است.

در برش بعد سوم یک گسله (عمود بر PDZ) علاوه بر سطح محوری چین‌های En-echelon و شیرینگ‌های R، ساختمان‌های گلواری نیز مشاهده می‌شود که بسته به همگرایی یا واگرا بودن گسله، این ساختمان‌ها به دو دسته ساختمان‌های گلواری مثبت و ساختمان‌های گلواری منفی تقسیم می‌شوند. Harding (1985) برپایه بررسی‌های خود روی مقاطع لرزه‌ای نشان داده که ساختمان‌های گلواری مثبت به صورت ساختمان‌های خطی طاقشکل هستند و حرکت رو به بالا دارند و به دلیل هندسه ساختمان‌شان که مناسب برای انباشته شدن نفت هستند، در اکتشاف نفت حائز اهمیت‌اند.

ساخت مدل‌های آزمایشگاهی از گسله‌های امتداد لغز ابتدا بوسیله Cloose (1928) با استفاده از رس آغاز شده است. (1970) Tchalenko ضمن ساخت مدلی از یک گسله امتداد لغز با استفاده از رس و جعبهٔ شیرینگ آن را با نمونه‌ای در طبیعت (گسله دشت بیاض در ایران) مقایسه کرده است. Naylor et al (1986) نیز در مدل خود با استفاده از ماسه ساختمان‌های مختلف حاصل از کارکرد این گسله‌ها را نشان داده است.

مدل باید از دیدگاه کینماتیکی، هندسی و دینامیکی با طبیعت همخوانی داشته باشد.

مدلی که در اینجا توصیف شده از نظر کینماتیکی با هر گسله امتداد لغزی در طبیعت که هیچگونه فرسایش و رسوب‌گذاری در حین و پس از تغییر شکل در آن صورت نگرفته است، قابل قیاس است. از نظر هندسی نیز هر یک میلی‌متر از مدل در همهٔ ابعاد برابر با ۱۰۰ متر در طبیعت است. از نظر دینامیکی، نسبت استرس مدل با طبیعت باید یک باشد. معادلهٔ استرس برای مدل و طبیعت به صورت زیر است:

$$\sigma = \rho g l \quad \text{که } \sigma \text{ استرس، } \rho \text{ دانسیته، } g \text{ شتاب جاذبه و } l \text{ طول است. با توجه به این که در مدل و طبیعت شتاب جاذبه برابر است}$$

$$\sigma_m / \sigma_p = \rho_m / \rho_p \quad l_m / l_p$$

Modelling Of Strike- Slip Faults

By: H. Shahrivar *

برای هرچه بیشتر شبیه شدن مدل با طبیعت باید از یک سری خواص بدون بعد فیزیکی مشابه استفاده کرد. در این نوشته ساختمان‌های گلووار مثبت حاصل از گسله امتدادلغز همگرا توسط ایجاد چند مدل مورد مطالعه قرار گرفته است. برای ساخت مدل‌های مورد بحث از دستگاهی مرکب از یک جعبه دنده یک الکتروموتور و جعبه شیرینگ (Shear Box) با ابعاد $20 \times 17 \times 7.5$ cm استفاده می‌شود (شکل ۱). ماده مورد استفاده نیز یک نوع ماسه است که در ابعاد کوچکتر از 0.2 میلیمتر دانه‌بندی شده و وزن مخصوص آن 1.4 g/cm^3 است. برای تفکیک بهتر لایه‌ها از میان- لایه‌های نازک ماسه به رنگ آبی و سیاه استفاده شده است. ضخامت لایه‌های سفید 5 میلیمتر است. جعبه مدل طوری آماده شده که در زیر آن دو صفحه قرار دارد که به صورت موازی به سمت هم حرکت می‌کنند. گسل در هر چهار آزمایش از نوع چپ رو است. در آزمایش اول و دوم مکانیزم عمل گسله شیرینگ محض است که با آن در لزای کوتاه‌شدگی چین‌های خوابیده پدید می‌آیند. در دو آزمایش دیگر مکانیزم عمل شیرینگ ساده است که در آن‌ها ساختمان‌های گلووار مثبت با ساختمان طاقشکل و حرکت رو به بالا پدید می‌آید.

Summary

According to Sylvester (1988) a strike slip fault is a fault on which most of the movement is parallel to the fault's strike. They could be 100 km in length and amount of displacement is between few millimeters to tens of kilometres. Geologically we have an echelon arrays of fractures, faults and folds in narrow zones. In addition strike slip faults displace structures like faults, folds, dikes, foliations, sills; they put rocks with different age, lithology, facies and structure near each other.

In strike slip faults there are three major structures: 1- Shortening; 2-Extension; 3- Horizontal shear.

Two mechanisms explain the geometric and dynamic relation among these faults and associated structures:

1- Pure shear; 2- Simple shear

The major strike slip faults of the world fall in the domain of simple shear (Sylvester 1988).

These faults have been studied by making models in experimental tectonic laboratories. Five sets of fractures form in simple shear in model experiments, experimental deformation of homogeneous rocks under confining pressure, and in alluvium deformed by surface rupturing during earthquakes (Sylvester 1988):

- 1- Riedel shears (R) at an angle of 30° with principal displacement zone (PDZ) and the sense of strike slipping is the same as PDZ (the first order structure).
- 2- Conjugate Riedel shears (R') at angle of $90^\circ - 30^\circ$ with (PDZ) and the sense of strike slipping is opposite to the PDZ.
- 3- P shears at an angle of 60° to the (PDZ) and the sense of strike slipping is the same as PDZ (the second order structure).
- 4- Extension fractures (T) which develop at about 45° to the PDZ.
- 5- Faults parallel (Y) to the PDZ.

Furthermore in the third dimension the axial surface of an echelon folds and riedel shears, flower structures can be observed, which depending on the direction of movement, they subdivide to positive and negative flower structures. As Harding (1985) shows in seismic profiles, a positive flower structure is defined as a linear antiform with upward and outward diverging movement of blocks in the strike slip zone. The antiform is sub parallel to and thereby differs from the oblique orientation of an echelon that can form externally to the zone, these initial antiforms in positive flower structures can be potential for hydrocarbon traps.

Experiments of strike slip faults started in 1928 by Cloos. Tchalenko (1968 and 1970) used shear box and clay to study the surface effects of strike slip fault and compared them with an example in natural example of "Dasht-e-Bayaz" fault (Iran). Naylor (1986) studied strike slip fault deformation in dry sand.

In order to apply model results to nature, model should be scaled kinematically, geometrically and dynamically to nature. Stress ratio for model and nature is;

For a model to simulate its natural prototype, a set of dimensionless ratios which relate the physical properties of model material and natural rocks should be similar (Koyi and Peterson 1993). Here 4 sand models are prepared and defined in order to study the geometry and kinematics of flower structures.

Introduction

Positive flower structures which occur in convergent strike-slip faults are available to oil exploration. Harding has studied positive and negative flower structures by seismic data (Harding 1973 and 1985).

Experiments of strike-slip faults started in 1928 by Cloos and 1929 by Riedel who used clay cake. Tchalenko (1968 and 1970) used shear box and clay to study the surface effects of strike-slip fault and compared them with an example in nature "Dasht-e-Bayaz" fault (Iran).

Because clay models may be applicable for the ductile lower crust and sand models are more appropriate to faulting in sedimentary rocks of the brittle upper crust (Naylor 1986) nowadays use of sand is preferred. Emons (1969) published his observation from surface and cross section during strike-slip faulting in sandbox. In cross section he observed upward movement of blocks over basement fault and referred to them as horst and graben. In map view he obtained shapes similar to Riedel shear and principal displacement zone (PDZ).

Naylor (1986) studied strike-slip fault deformation in dry sand and observed (R) Riedel shears, (S) splay faults, (P) secondary synthetic shears and (Y) shears parallel to the (PDZ). In cross section, he showed two concave upward basement faults diverging from the basement fault forming a tulip structure. In addition he concluded that the width and complexity of the strike-slip is determined by the total basement displacement, the initial stress state, and pure strike-slip displacements generate concave upward faults arranged in tulip structure, convex upward fault in

the form of palm tree structure depend to transpression or strike-slip movement on steeply dipping basement fault.

Here 4 sand models are prepared and defined in order to study the geometry and kinematics of flower structures.

Strike-slip faults

A strike-slip fault is a fault on which most of the movement is parallel to the fault's strike. They could be 1000 Km in length and amount of displacement is between few millimeters to tens of kilometers (Sylvester 1988).

Clearly all wrench, transcurrent and transform faults are by geometry strike-slip faults (Freund 1974). Term wrench fault is used for a deep seated, regional, nearly vertical strike-slip fault which involves igneous and metamorphic basement rocks as well as supracrustal sedimentary rocks (Sylvester 1988). Transform fault is used for a plate bounding strike-slip fault and transcurrent fault is the general term for the variety of strike-slip fault which do not cut the lithosphere (Sylvester 1988). Freund (1974) has listed the differences between transform and transcurrent faults.

Geologically we have an echelon arrays of fractures, faults and folds in narrow zones. In addition strike-slip faults displace structures like faults, folds, dikes, foliations, sills and put rocks with different age, lithology, facies and structure near each other.

Mechanism of strike-slip faults

In strike-slip faults there are three major structures

- 1- Shortening
- 2- Extension
- 3- Horizontal shear

These structures have three main aspects in common:

- 1- The en echelon nature of folds and faults
- 2- Complication due to components of reverse or normal dip-slip on the basement fault.
- 3- Lateral offsets of basement involved strike-slip faults which create local extensile or shortening structures (Sylvester 1988).

Two mechanisms explain the geometric and dynamic relation among these faults and associated structures

- 1- Pure shear
- 2- Simple shear

Pure shear produces relatively short, typically conjugate sets of strike-slip faults which help to accommodate the brittle component of strain in tectonic regimes of crustal shortening such as over thrust belts. Extension fractures will form perpendicular to elongation axis and shortening structures are perpendicular to the shortening axis (Sylvester 1988).

The major strike-slip faults of the world are in domain of simple shear (Sylvester 1988).

Five sets of fractures form in simple shear in model experiments, experimental deformation of homogeneous rocks under confining pressure, and in alluvium deformed by surface rupturing during earthquakes (fig.1) (Sylvester 1988).

- 1- Riedel shears (R) at an angle of ϕ with principal displacement zone (PDZ) and the sense of strike-slip is the same as PDZ (the first form structure).
- 2- Conjugate Riedel shears (R') at angle of $90^\circ - \phi$ with (PDZ) and the sense of strike-slip is opposite to the (PDZ).
- 3- P shears at an angle of $\frac{\phi}{2}$ to the (PDZ) and the sense of strike-slip is the same as (PDZ). (The second order structure).
- 4- Extension fractures (T) which develop at about 45° to the (PDZ).
- 5- Faults parallel (Y) to the (PDZ).

Folds and thrust faults form initially perpendicular to the axis of shortening and at angle of 45° to the PDZ (Fig. 2). If deformation continues then the fold axis will rotate according to the amount of shearing. Folds associated with strike-slip faults are typically arranged in an echelon pattern oblique to the principal direction of shear. These folds are distributed in narrow and persistent zones above or adjacent to a master strike-slip fault or broad zones between two major strike-slip faults. These folds received much attention from the petroleum industry (Sylvester 1988).

Structures in cross section

In three dimension, the axial surface of en echelon folds in a sequence of strata overlying a rigid basement are nearly vertical

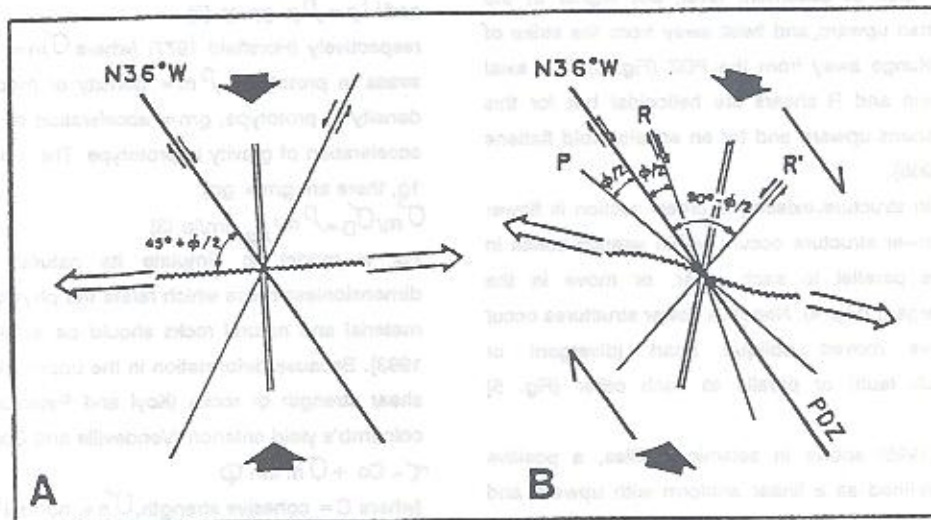


Figure 1. Plan view of geometric relations among structures according to two dimensional strike slip. (A) Coulomb - Anderson model of pure shear, (B) Riedel model of right simple shear. from Sylvester (1988).

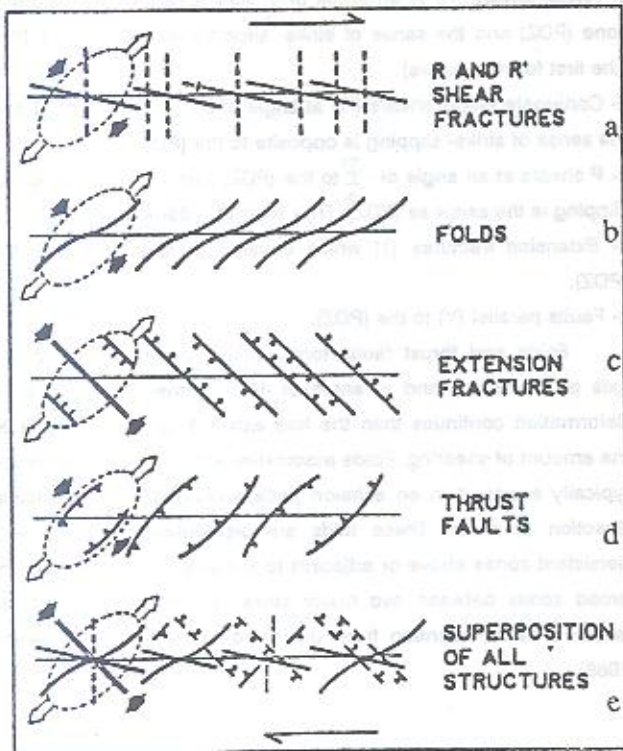


Figure 2. Orientation of folds and faults in bulk right simple shear (from Sylvester 1988).

and parallel to the fault at basement level, but higher in the overburden they flatten upward and twist away from the strike of the fault and they plunge away from the PDZ (Fig. 3). The axial surface of an echelon and R shears are helicoidal but for this surface R shear steepens upward and for an echelon fold flattens upward (Sylvester 1988).

The other main structure existing in cross-section is flower structure. Positive flower structure occurs within wrench zones in which block moves parallel to each other, or move in the component of convergent (Fig. 4). Negative flower structures occur where blocks have moved oblique apart (divergent or transtensional wrench fault) or parallel to each other (Fig. 5) (Harding 1985).

As Harding (1985) shows in seismic profiles, a positive flower structure is defined as a linear antiform with upward and outward diverging movement of block in the strike-slip zone. The antiform is sub parallel to and thereby differs from the oblique orientation of an echelon that can form externally to the zone (Fig. 6).

These initial antiforms in positive flower structures can be

potential for hydrocarbon traps, and they are not as attractive hydrocarbon prospects as the less intensely deformed en echelon folds (Harding 1985).

The formation of flower structure is promoted by a component of convergence normal to the wrench fault, by increased strike-slip displacement and by the presence of a thick and ductile sedimentary section (Harding 1985). Harding (1985) also shows the divergent component of the shearing which promoted a brittle fault in Andaman Sea (Indonesia) (Fig. 7). In this example the drape flexures face each other across the fault and they define a shallow synform "negative flower structure" that also strikes sub parallel to the zone. This feature is termed a synform because it may resemble a syncline only in morphology.

The differentiation of negative and positive flower structure should not be difficult because of the obvious differences and the presence of shallow synforms or antiforms respectively.

Scaling: In order to apply model results to nature, model should be scaled kinematically, geometrically and dynamically to nature. The model described here is scaled kinematically to any strike-slip fault in nature which has no sedimentation and erosion during or after deformation. Geometric scaling was achieved by scaling vertical and horizontal distances in model and nature giving the length ratio of 10^{-5} , it means that 1mm in the model simulates 100m in nature. In order to achieve dynamic similarity the stress ratio acting on model and nature should be equal to one.

$$\sigma_m = \rho_m \cdot g_m \cdot l_m \quad (1)$$

$$\text{and } \sigma_p = \rho_p \cdot g_p \cdot l_p \quad (2)$$

respectively (Horsfield 1977) (where σ_m = stress in model, σ_p = stress in prototype, ρ_m = density of modelling material, ρ_p = density of prototype, g_m = acceleration of gravity in model, g_p = acceleration of gravity in prototype. The models were deformed at 1g, there are $g_m = g_p$).

$$\sigma_m / \sigma_p = \rho_m / \rho_p \cdot l_m / l_p \quad (3)$$

For a model to simulate its natural prototype, a set of dimensionless ratios which relate the physical properties of model material and natural rocks should be similar (Koyi and Peterson 1993). Because deformation in the upper crust is controlled by the shear strength of rocks (Koyi and Peterson 1993) We use from Coulomb's yield criterion (Vendeville and Cobbold 1988):

$$\tau = C_0 + \sigma_n \cdot \tan \phi$$

(where C_0 = cohesive strength, σ_n = normal stress and ϕ = angle of internal friction τ = shear stress)

then we will have following ratios (Wijermars 1993)

$$\sigma_m / \sigma_p = l_m / l_p \cdot \rho_m / \rho_p = C_m / C_p \quad (5)$$

$$i_{p/m} \rho_m = 1.4 \text{ g Cm}^{-3} \text{ and } \rho_p = 2.6 \text{ g Cm}^{-3} \quad \rho_m / \rho_p = 0.54 \text{ and } l_m / l_p = 10^{-5}$$

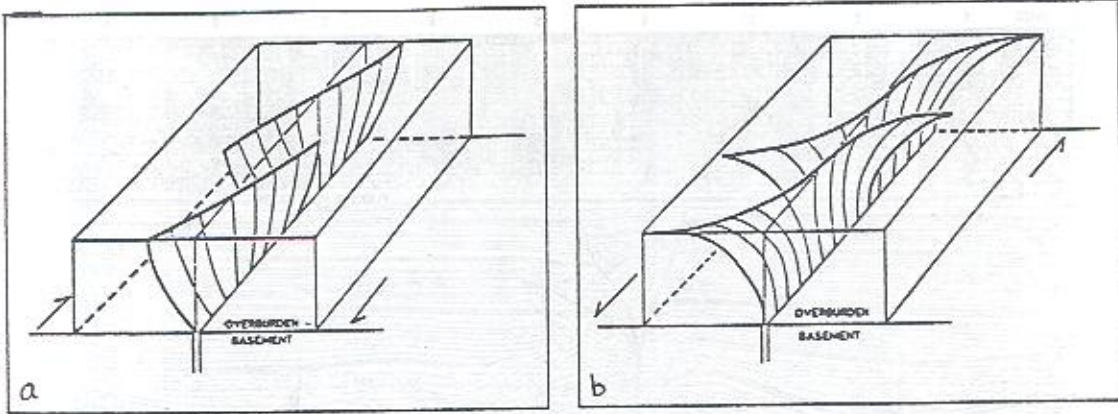


Figure 3. Helicoidal form of (a) Riedel shear and (b) en echelon fold. (from Syllvester 1988).

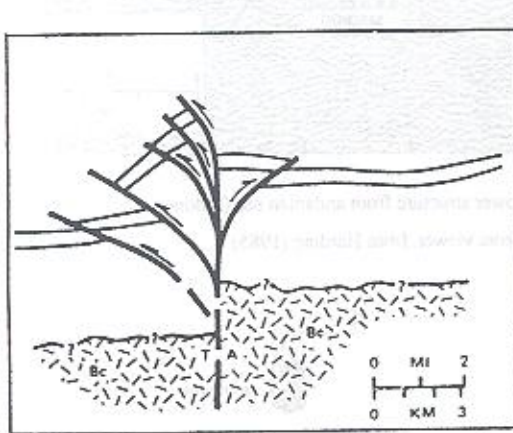


Figure 4. Positive flower structure. (A) away from viewer (T) toward viewer. From Harding (1985).

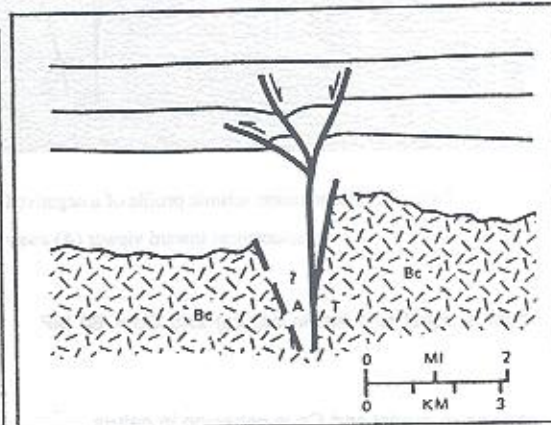


Figure 5. Negative flower structure (A) away from viewer (T) toward viewer (from Harding 1985)

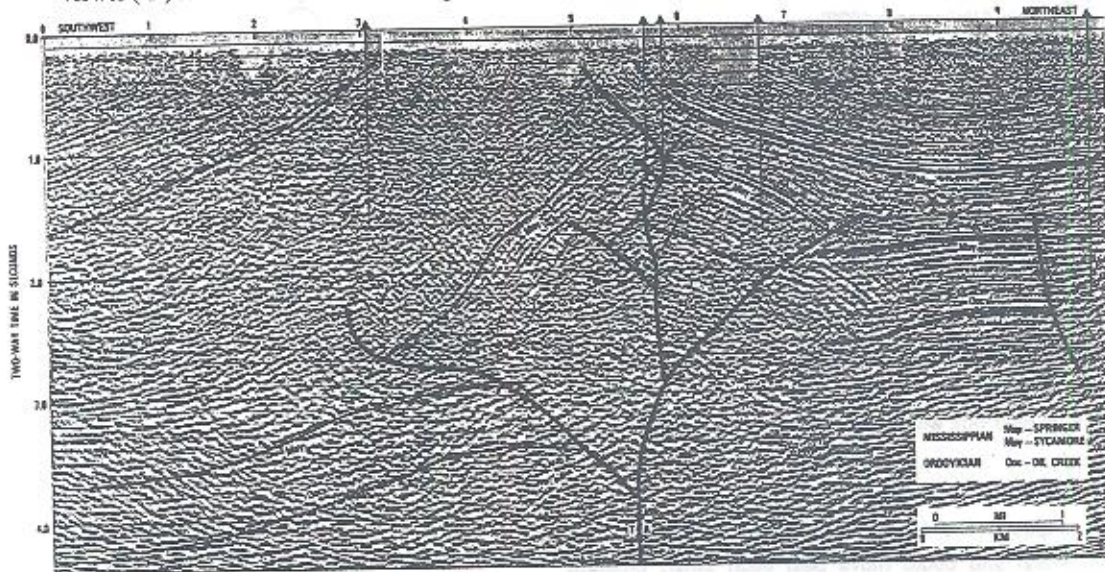


Figure 6. Interpreted seismic profile of a positive flower structure across convergent wrench zone in Andomor basin California (T) displacement toward viewer (A) away from viewer. from Harding (1985).

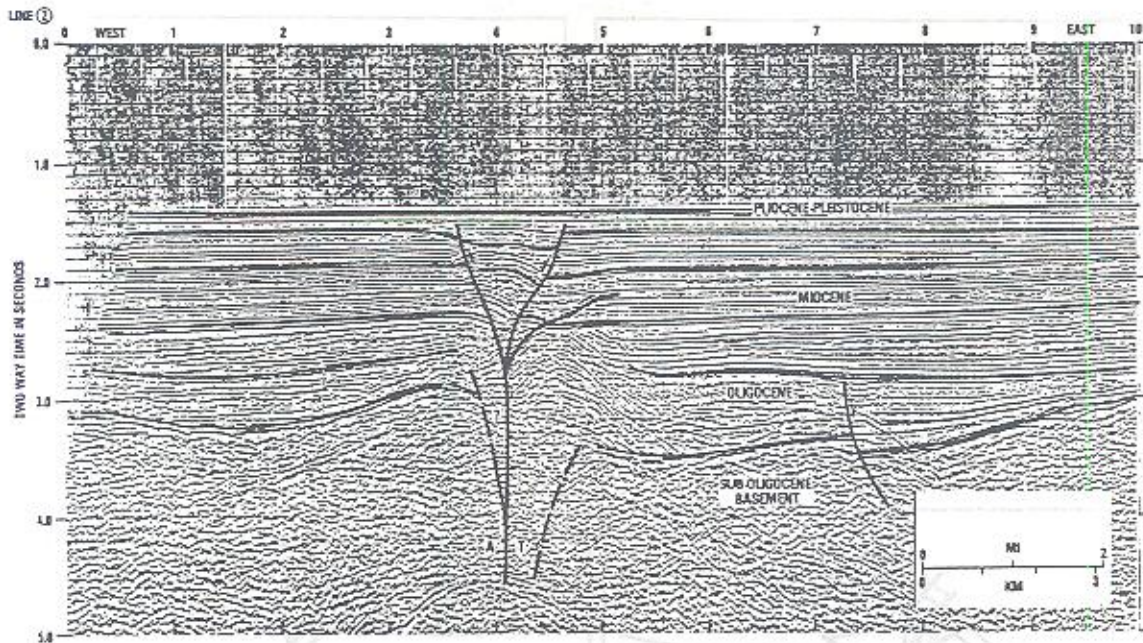


Figure 7. Interpretation seismic profile of a negative flower structure from andaman sea (Indonesia). (T) displacement toward viewer (A) away from viewer. from Harding (1985)

if P_m (1 Cm model is equal to 1 km in nature) and $C_p = 60 \text{ MP}$ then
 $C_m = 300 \text{ Pa}$
 Where C_m is cohesion in model and C_p is cohesion in nature.

Range of cohesion in sandbox shows variation between 0-300 Pa, with further compaction increases although cohesion in dry sand is negligible (Weijermars 1993).

Friction coefficient is between 0.6 to 0.86 in natural rocks shallower or deeper than 10 Km respectively and angle of internal coefficient is 22° to 41° (Weijermars 1993). Coefficient of internal friction in the model and nature must be equal (Koyi and Peterson 1993).

Modelling

Apparatus: An old gear box was used to deform the models (Fig. 8). the box consisted of the following parts.

- 1- An electric motor, 220 Volt, 1.4 HP, 1560 Rpm.
- 2- An automobile gear box with five gears four to the front and the fifth to the back.
- 3- shear box with 20 Cm length, 17 Cm width and 7.5 Cm height, Shear box composed two L shape on which the model were placed (containers) and could move past each other. Different containers with different sizes were used.

Modelling material: Dry sand with grain size ($< 0.2 \text{ mm}$)

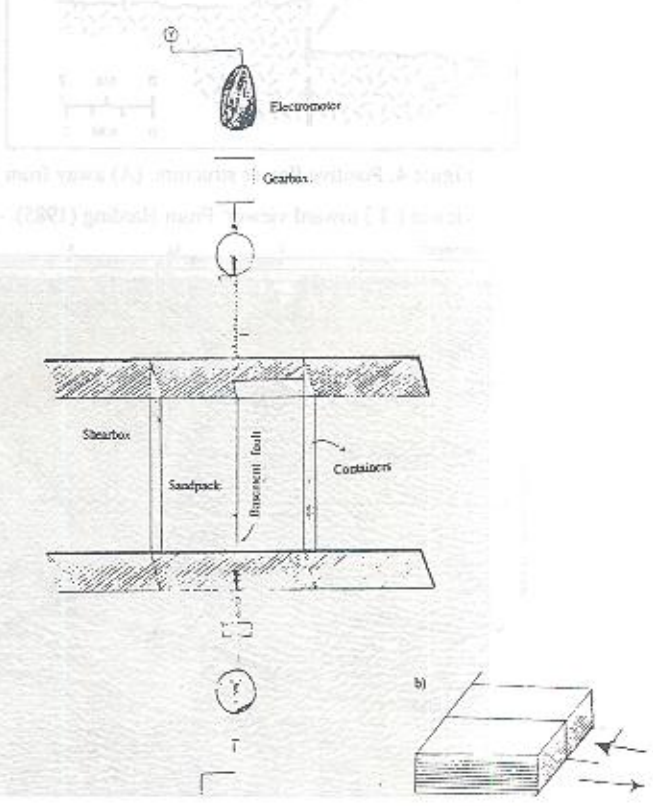


Figure 8. Perspective of a) apparatus , b) Sand pack .

and density (ρ) of 1.4 g Cm^{-3} was used. For colour contrast between layers blue and black sand were used.

Preparation of model: White layers with 5mm thickness were placed in box and thin coloured layers were put between them as strain markers.

Deformation procedure: Here layers of loose sand are deformed in a box (Fig.1). The sand layers were placed on the plates (which moved parallel to each other). The two plates were moved on opposite direction parallel to each other.

Experiments: Four experiments have been done and reported here, movement was left handed, Table 1 shows modelling and deformation parameters. Each white layer was 5mm. and sedimentation was horizontal (except exp. no. 4), blue and black sand used as intralayers.

Number of exp.	H - 1	H - 2	H - 3	H - 4
h(cm)	6	6	4.5	6
l(cm)	22.7	21	19.3	19.3
l_1 (cm)	17.1	14.9	14.7	15
T(mm)	5	5	5	5
t (s)	2140	1800	1750	1660

Table 1. Specification of the used sandbox to deformation the models, where h is thickness of sand pack, l is length of shear box, l_1 is length of shear box after deformation, T is thickness of each layer and is time.

Model results

Experiment no. 1

8 layers of white sand of 5mm thick were separated by a thin layer (1mm) of blue sand put in the box (fig.9) Fig. 10 shows a 3-D view of a deformed model, sand is mixed with wet glue to have stability for cutting, in this case angle of internal friction is high and cohesion is not negligible, Conjugate box folds produced near the compression plates also direction of movement can be defined by inclined asymmetric folds. Amount of shortening is about 24% for 36 minutes

Experiment no.2

This model contained dry sand with blue and black intralayers. The model was deformed in pure shear and shortened by 29% for 30 min. which is faster than model no.1. Figure 11 shows a section perpendicular to the direction of movement, recumbent folds, sheath folds. Displacement of block between two fault is upward in contrast with down ward movement which is

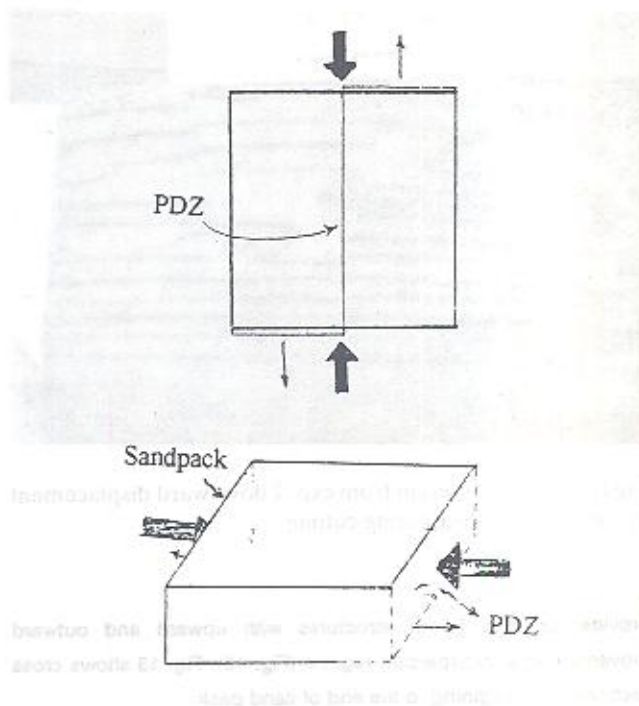


Figure 9. Arrangement of sandbox in exp. no. 1 and 2 bold arrows show movement of compression and small arrows show free places to escaping containers.

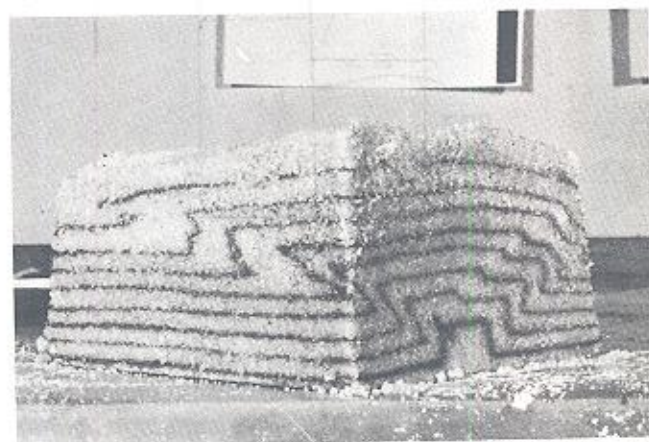


Figure 10. Model in pure shear, which one is direction of movement ?

effect of moving and cutting the sand pack.

Experiment no.3

Container filled with 8 horizontal white layers and blue intralayers. Instead of having pure shear, plates move in this model past each other in simple shear. This strike-slip movement

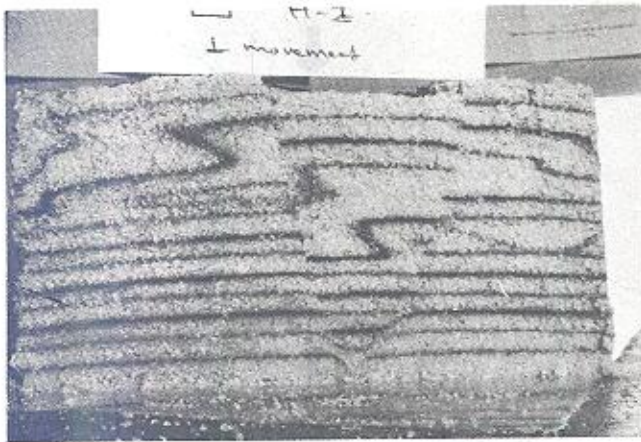


Figure 11. Cross section from exp. 2 downward displacement of the block is effect during cutting

provides positive flower structures with upward and outward movement in a transpersion regime (Fig. 12). Fig. 13 shows cross sections from beginning to the end of sand pack.

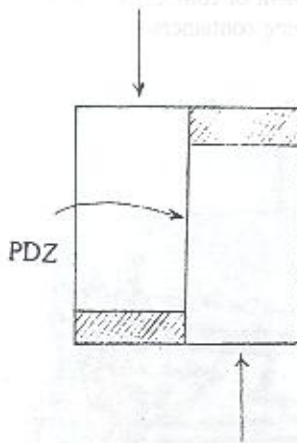


Figure 12. Plan view of sandbox, arrows show direction of movement and hatching are prepared space for pure strike slip.

Experiment no. 4

Like exp. 3 apparatus installed (Fig.12) instead of having horizontal layers, for clear observation of upward displacement second and third layers were deposited with opposite slope. Fig. 14 shows four stage of shortening from top view, principal displacement zone with upward movement including synthetic shears (R) is visible. Fig. 15 shows three section of this model.

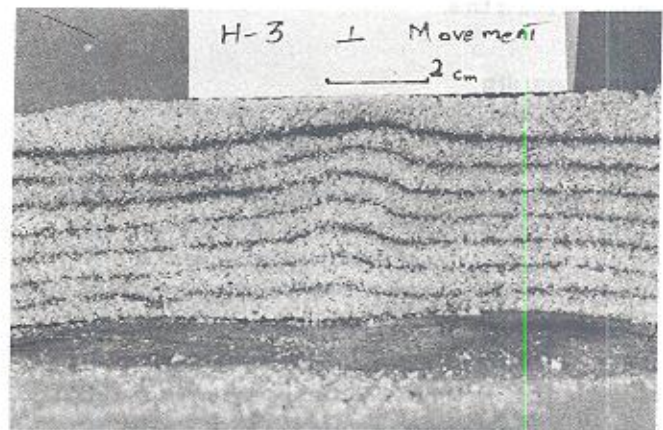
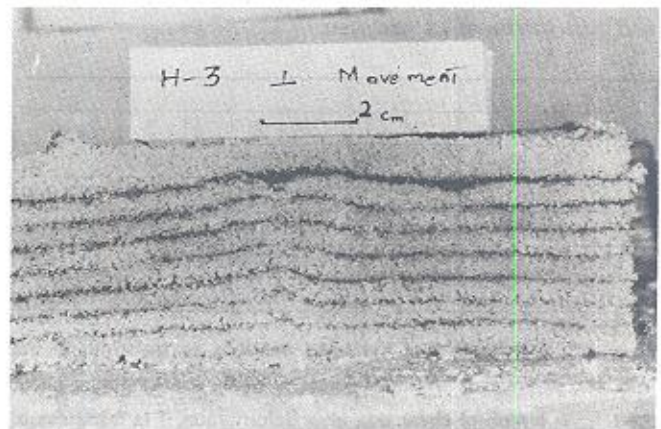
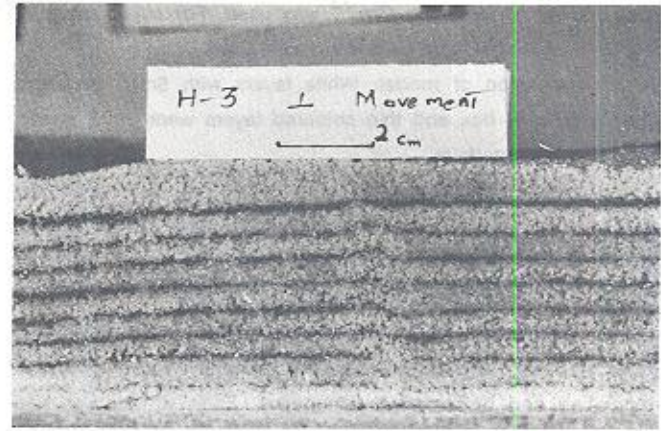


Figure 13. (a.) Antiform shape of black layers are obvious, rate of bending in the left fault in flower structure is more than the right because the left part of model is coming toward viewer, on the other hand direction of sliding can be find; (b). cross section near (a) shows middle part of sand pack but bending is not clear as is seen in (a); (c) shows section from inside of pack, but opposite to (a) bending is asymmetric and the part which is going aoward viewer is more banded, thicker part in the upper black layer (which is deposited after deformation) shows PDZ.

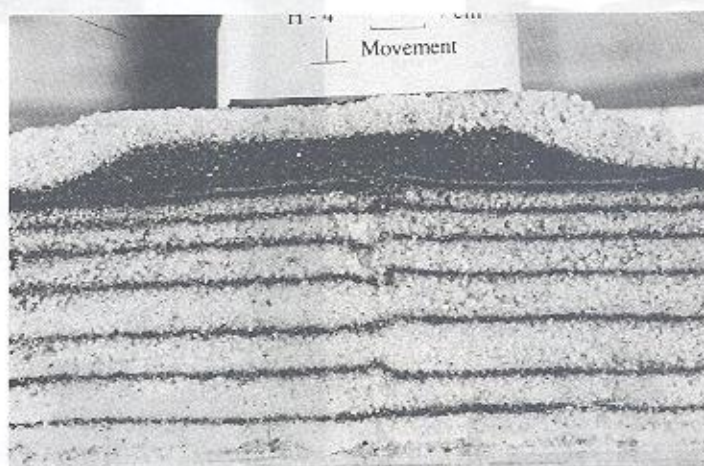
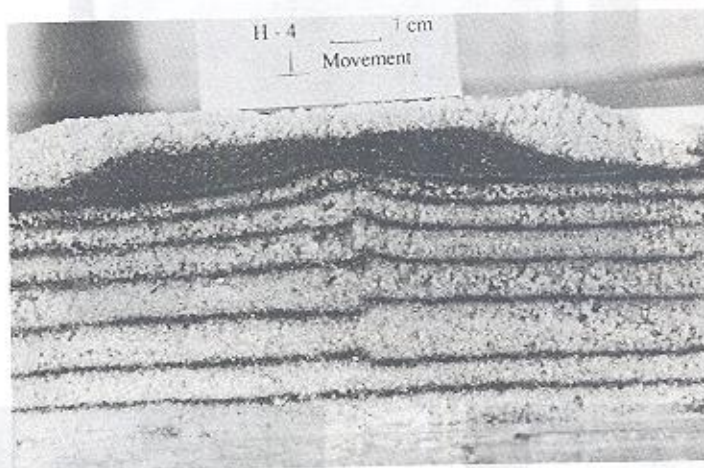
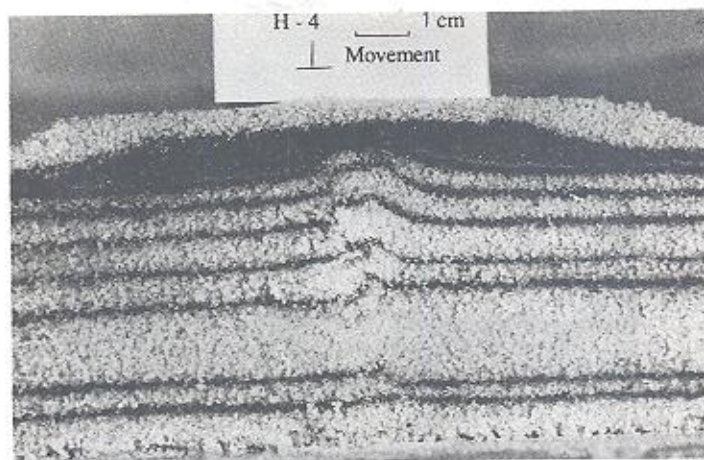


Figure 14. (a) shows middle part of PDZ and asymmetric bending in fault block, in the left side kinking is near vertical and in right is gentle, upper thick black layer which is post deformation shows surficial effect of gliding which has come in fig. 15; (b) is from the middle part near the end, now bending in the right side is near vertical; (c) from end of deformed sand pack, upward movement is not same as (a) because this section is near the end of PDZ.

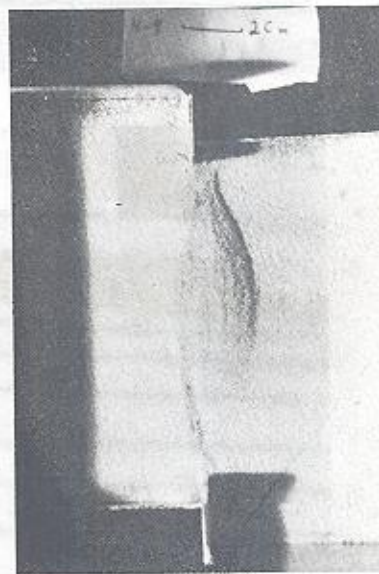
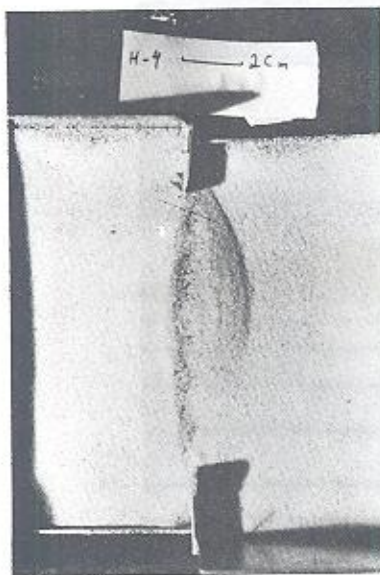
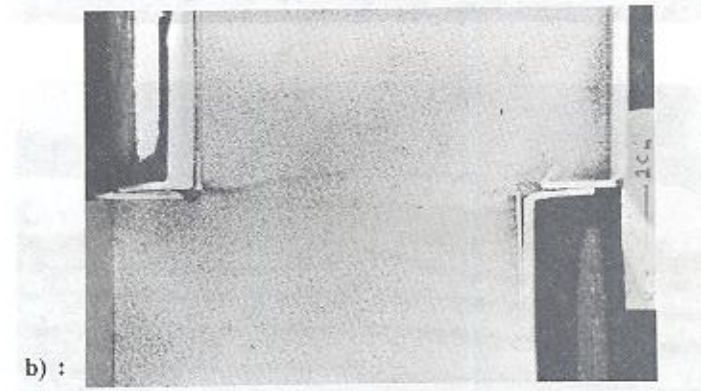
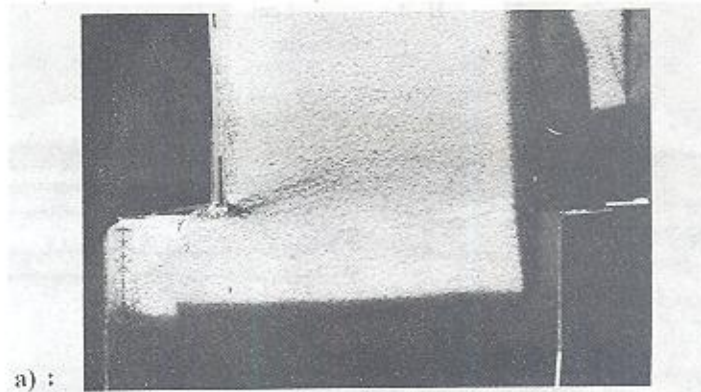


Figure 15. Top view from beginning to end of exp. no. 4, note to the PDZ, asymmetric upward movement.

Conclusion

Pure shear is the main mechanism of experiments 1 and 2. Inclined and recumbent folds compensate component of shortening. Flower structures which have occurred in pure strike-

slip (experiments 3 and 4) were antiform and had upward movement. Asymmetric shape of these bedded layers shows direction of movement.

Acknowledgement

This report presents the study carried out at the Hans Ramberg Tectonic Laboratory at Uppsala University. Thanks are due to Prof. C. J. Talbot for his guidance, Dr. H. Koyi for his supervising and commenting on this report and E. Meland for preparing the necessary facilities required for the experiment. I also thank Dr. M. Alavi for his reviewing on farsi summary. This is contribution no. 5 of the Research Institute for Earth Sciences, GSI.

References

- Cloos, H. 1928. Experimente zur innera tektoniczentribiatt fur mineralogie und paleontologie v. 1928, p. 609-621.
- Emone R. C. 1969. Strike- slip rupture patterns in sand model. *Tectonophysics*, V. 7, p. 71- 87.
- Ferund R. 1974. Kinematics of transform and transcurrent faults. *Tectonophysics*, V. 21, P. 93- 134.
- Harding T. P. (1973). New port- Ingelwood trend, California- An example of wrenching style of deformation. *AAPG Bulletin*, V 57 (1), p. 97- 116.
- Harding T. P. 1985. Seismic characteristics and identification of negative flower structures and positive flower structures and positive structural inversions. *AAPG Bulletin*. V. 69, p. 582- 600.
- Horsfield W. T. 1977. An experimental approach to basement controlled faulting. In *fault tectonics in NW Europe* . Edited by Frost R. T. C. and Dikkers A. J. *Geologie mijnb.* 56, 363- 370.
- Koyi H. and Peterson K. 1993. Development of salt structures in the Danish Basin. *Marine and petroleum geology*. V. 10 Apr.
- Mullugeta G. and Koyi H. Episodic accretion and strain partitioning in a model sand wedge. *Tectonophysics*. V. 202, p. 319- 333.
- Naylor M. A., Mandl G. and Sijpestijn C. H. K. 1986. Fault geometries in basement induced wrench faulting under different initial stress. *Journal of structural geology*. V. 8, p, 737- 752.
- Sylvester R. G. 1988. Strike- slip faults: *GSA Bulletin* V. 100, p. 1668- 1703.
- Tchalenko J. S. and Amberseys N. N. 1970. Structural analysis of the Dasht- e Bayaz (Iran) earthquake. *GSA Bulletin*. V. 81, p. 41- 66.
- Vandeville B. and Cobbold P. R. 1988. How normal faulting and sedimentation interact to produce listric fault profiles and stratigraphic wedges. *Journal of structural geology*. V. 10- No. 7, p. 649- 659.
- Weijermars R., Jackson M. P. A. and Vandeville B. 1993. Reological and tectonic modelling of salt provinces. *Tectonophysics*. V. 217, p. 143- 174.

* Geological Survey of Iran

پژوهشکده علوم زمین، سازمان زمین شناسی کشور